Molecular Crystals and Liquid Crystals

Publication details, including instructions for authors and subscription information:
http://www.tandfonline.com/loi/gmcl16

Heat Convection in a Nematic Liquid Crystal

E. Dubois-violette [a], E. Guyon [a] & P. Pieranski [a]

[a] Laboratoirt de Physique des Solides. Université Paris-Sud, Centre d'Orsay, 91405, Orsay

Version of record first published: 21 Mar 2007.

To cite this article: E. Dubois-violette , E. Guyon & P. Pieranski (1974): Heat Convection in a Nematic Liquid Crystal, Molecular Crystals and Liquid Crystals, 26:3-4, 193-212

To link to this article: http://dx.doi.org/10.1080/15421407408083099

Mol. Cryst. Liq. Cryst., Vol. 26, pp. 193-212

Printed in Dordrecht, Holland

Heat Convection in a Nematic Liquid Crystal

E. DUBOIS–VIOLETTE, E. GUYON and P. PIERANSKI

Laboratoire de Physique des Solides‡,
Université Paris-Sud, Centre d'Orsay,
91405 Orsay

(Received November 11, 1972; in revised form March 30, 1973)

We present a theoretical and experimental study of the thermal properties of a well aligned nematic Liquid Crystal in a vertical temperature gradient. Due to the long time constant of the relaxation of the director and to the anisotropy of the heat conductivity, the value of the temperature gradient threshold for convective instabilities is strongly modified as compared to the isotropic case. Experiments on planar MBBA films show a drastic reduction of the threshold. A detailed description of the shape and temperature distribution of the convective rolls is given.

INTRODUCTION

The transport properties of a well aligned nematic liquid crystal (LC) film are strongly anisotropic. We consider here the thermal behavior of such materials both from the theoretical point of view and from experiments on MBBA (P methoxy benzilidene $p-n$ butylaniline). The thermal conductivity anisotropy is noted $k_a = k_{//} - k_\perp$ where // and $\perp$ refer to the orientation of the thermal gradient ∇T with respect to the director axis of the molecule $\underset{\sim}{n}$.

The most direct determination of k_a uses the comparative measurement of the temperature difference ΔT_z across single crystal LC films oriented parallel

† Presented at the Fourth International Liquid Crystal Conference, Kent State University, August 21–25, 1972.

‡ Laboratoire associé au C.N.R.S.

(planar) and perpendicular (homeotropic) to the walls of the cell ($z = 0, d$). Our results[1] on rather thick films ($d = 200$ to $500\ \mu$) have led to an anisotropy ratio

$$k_{//}/k_{\perp} = 5/3$$

Another determination uses the distortion of the LC in a magnetic field perpendicular to the film above the Freedericksz threshold H_c. If the heat flow through the LC is kept constant, the temperature gradient is found to increase in an homeotropic sample (to decrease in a planar sample) when a field $H > H_c$ is applied. Using the known expression of the distortion angle

$\theta\ (z)$ (we use the notations of (1))

and $k\ (\theta) = (k_{\perp} + k_a \sin^2\theta)$ Planar

$= (k_{//} - k_a \sin^2\theta)$ Homeotropic

We got a good description of the Freedericksz transition and a value of the ratio

$$k_{//}/k_{\perp} = 1.6 \pm 0.15$$

in agreement with the direct determination quoted above.

Comparable data have been obtained on P.A.A. by Longley-Cook and Kessler[2,3] on magnetically aligned samples. Previous experiments with samples of incompletely defined orientation had led to contradictory results (a review of these results can be found in (3)). In particular, a coupling between the heat flow and molecular orientation[4,5] has been reported in some cases. This coupling was observed only in experiments with a vertical temperature gradient. The possibility of a convection driven mechanism was eliminated on the ground that ΔT was smaller than the threshold given in terms of a dimensionless Rayleigh number R_{cr}. In the next chapter, we will analyse the heat convection mechanism in LC and will see that the convective instability mechanism is quite different from that in isotropic materials and can lead to drastically reduced thresholds. Our experiments on MBBA reported in Chapter 3 will provide an experimental description of this effect on MBBA.

THEORY OF THE CONVECTIVE INSTABILITIES

Isotropic liquid

The hydrodynamic instabilities present in ordinary liquids heated from below have been extensively studied since the observations done by Benard in 1900.[6,7]

In a fluid film limited by solid surfaces, they appear above a threshold given by $R_{cr} = 1740$, where the dimensionless Rayleigh number is

$$R_I = \frac{\Delta T d^3 \rho g \alpha}{\kappa \eta}$$

The destabilizing upward buoyancy force $\rho g \alpha \Delta T$ on the hot lower layers of liquid is proportional to the value of the thermal expansion coefficient α.

The heat diffusivity $\kappa = \frac{k}{\rho C}$ (C = specific heat), which tends to prevent an horizontal modulation of the temperature associated with the periodic convection, and the viscosity η act as stabilizing mechanisms. In a typical liquid comparable to M.B.B.A.

$$\kappa \simeq 10^{-3} \text{ cm}^2/\text{s}, \eta \simeq 1 \text{ Poise and } \Delta T_{cr} \simeq 2^0\text{C} \quad \text{for } d = 1 \text{ cm}$$
$$\Delta T_{cr} \simeq 2.10^3 \text{ }^0\text{C for } d = 1 \text{ mm}$$

Mechanism in a LC

The situation is quite different in a LC: in addition to the Bénard process, there exists a specific mechanism due to the anisotropic properties of the LC phase. This anisotropic mechanism is the dominant one and the threshold is modified in ordered films. In particular, a new type of convective instability is predicted for a sample with a negative value of k_a.

Let us first analyse this mechanism qualitatively. As explained in Refs. 8 and 9, the effect of the thermal conductivity anisotropy k_a of the liquid crystal is very similar to the Carr–Helfrich process.[10,11] We consider a nematic sample, sandwiched between two places, in which a thermal gradient $\nabla T_z = -\beta$ is applied by heating the sample from below (Figure 1).

We suppose that the LC is initially oriented with the molecules along Ox (planar case) and we consider a fluctuation of the director orientation characterized by the angle $\phi(x)$ between $\underline{n}$ and Ox. (The thermal fluctuations of oriented liquid crystals are very reduced in the case of strong anchoring at the boundaries and are negligible in the case discussed here (see the second part of Ref. 1). Due to the thermal conductivity anisotropy, the heat flux lines are not perpendicular to the plates but are deviated:

a) along the molecules if $k_{//} > k_\perp$

b) perpendicular to the molecules if $k_\perp > k_{//}$

Warmer (2) and cooler (1) regions appear. The gravity forces induce opposite hydrodynamic velocities in regions 1 and 2. The viscous torque, due to the velocity gradient, is destabilizing in case (*a*) and stabilizing in case (*b*). In the

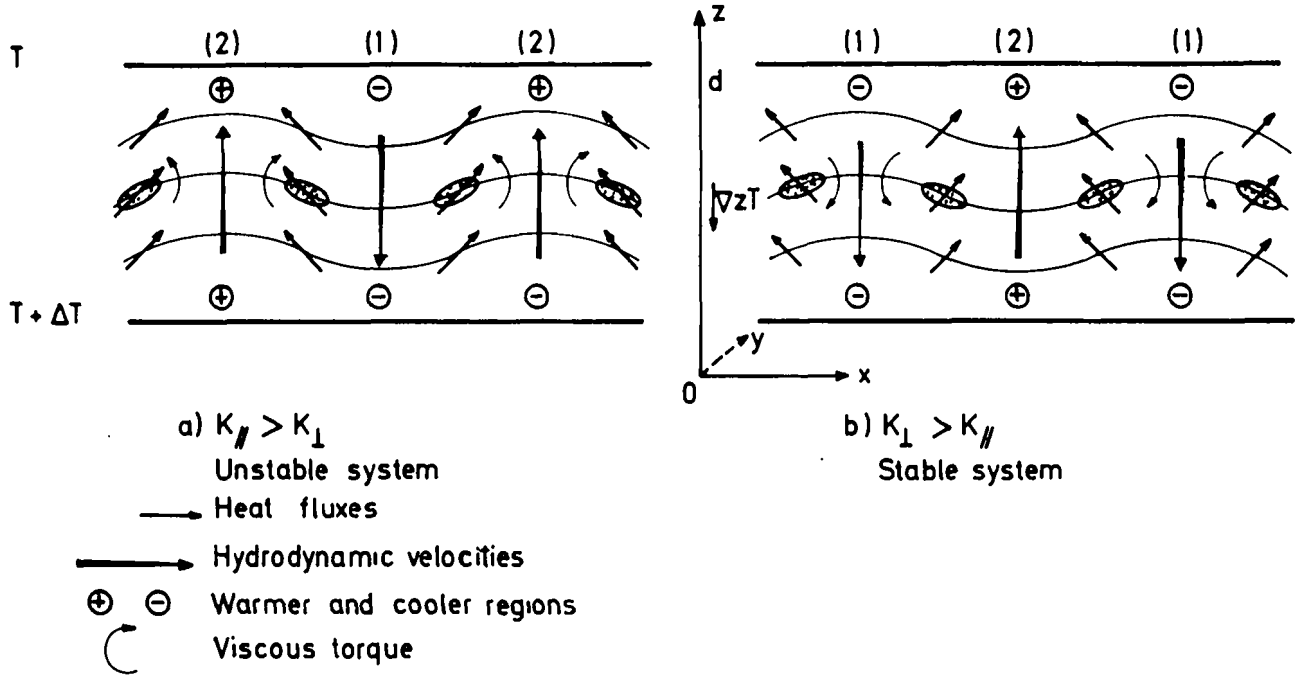

FIGURE 1 The nematic sample, initially in a planar configuration with the molecules parallel to Ox, is submitted to a thermal gradient $\nabla_z T$. The underside is maintained at temperature $T + \Delta T$, the upperside at temperature T. Due to the thermal conductivity anisotropy κ_a warmer (+) and cooler regions (−) appear. The viscous torque due to the anisotropic mechanism is destabilizing in case (*a*) and stabilizing in case (*b*).

first case (a), one expects an instability when the destabilizing viscous torque is larger than the stabilizing elastic torque. On the contrary, in case (b) where the viscous torque is stabilizing, the convection is strongly impeded. (Of course, the Bénard instability will appear for $k_a = 0$. But the LC stabilizing effect will be dominant typically as soon as $k_a > 10^{-6}$ *cgs*). Let us suppose now that the sample is heated from above (Figure 2). From similar arguments, one predicts that:

a) the system is stable if $k_{//} > k_{\perp}$

b) the system is unstable if $k_{\perp} > k_{//}$

The latter case, where we expect convective instabilities by heating the sample from above, is of course characteristic of the properties ($k_a < 0$) of the liquid crystal phase.

Thermohydrodynamic equations

We use the same model and notations as in Ref. 11:

– we assume that all quantities depend only on x and not on y or z. This assumption is justified since the dominant viscous torque depends on the velocity derivative $\frac{\partial V_z}{\partial x}$: In most nematics $\gamma_1 \sim -\gamma_2$ and the torque $\frac{\gamma_1 - \gamma_2}{2} \frac{\partial V_z}{\partial x}$ exerted on the molecules by the component of the fluid velocity perpendicular to the molecules is much larger than the torque $\frac{\gamma_1 + \gamma_2}{2} \frac{\partial V_z}{\partial x}$ due to the component parallel to the molecules.

A complete two dimensional model taking into account the x and z dependence would be needed in order to obtain the optimal wave vector of the distortion along Ox, as was done by Penz in the electrohydrodynamic case. However, we will use here the same assumption the one that we used in the electrohydrodynamic case[11] and take the distortion wavelength of the order of the sample thickness as justified experimentally. This is known to reproduce the two-dimensional calculation well in the electrohydrodynamic case.

– We consider small fluctuations $\delta \underline{n}_z(x)$ of the director $\underline{n}(x)$ characterized by the angle $\phi(x) = \phi_0 \cos(k x) e^{st}$. Only lowest order terms in ϕ will be retained in the equations.

This approximation is correct as we are only concerned with the infinitesimal distortions right above the threshold.

– we neglect, as in the Boussinesq[12] approximation, the density variations induced by δT except in the buoyancy force (δT is the temperature fluctuation induced by the fluctuation of orientation $\delta\phi$). This is justified because of the small value of the thermal expansion coefficient α ($\simeq 10^{-3}$ to 10^{-4} C^{o-1}). Parame-

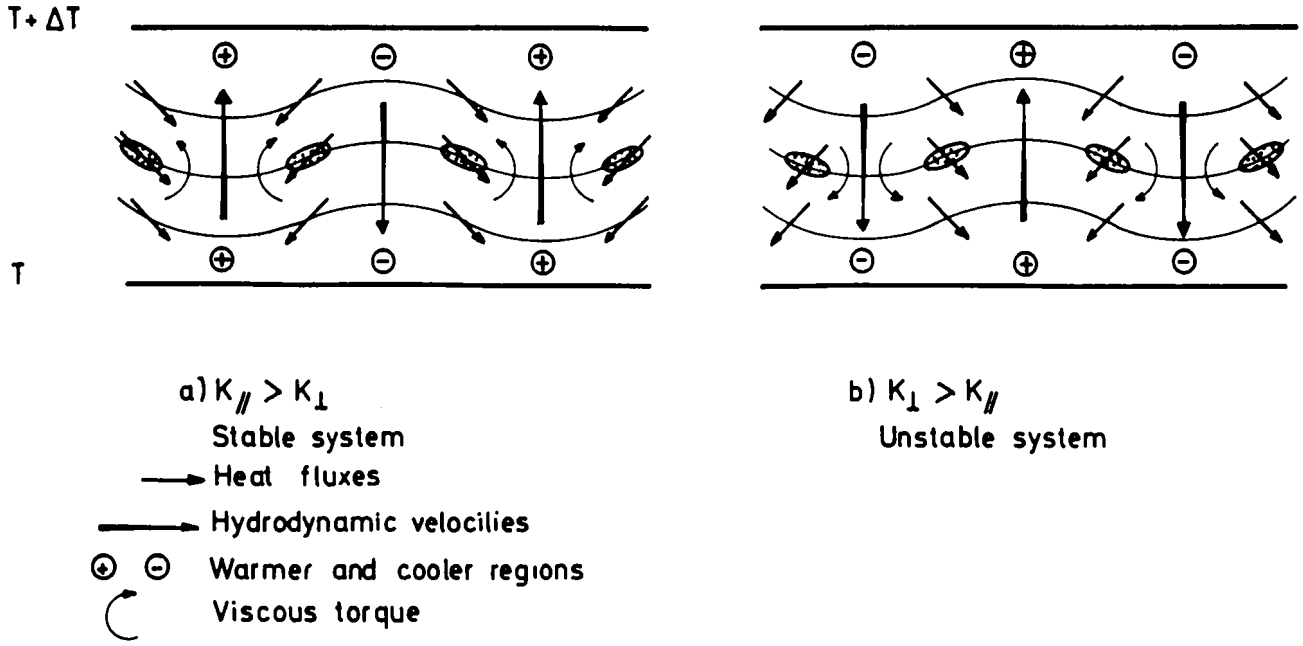

FIGURE 2 The nematic sample is heated from above. Case *b* corresponds to an unstable system since the viscous torque induced by the anisotropic mechanism is now destabilizing.

ters such as viscosities, specific heat C, conductivities are considered independent of T.

From the conservation laws, we obtain the four following equations:

Mass conservation equation

Let

$$T_i(z) = T_o - \beta z$$

be the initial temperature. The density $\rho(T')$ at temperature T' is related to the density $\rho(T)$ at temperature T by:

$$\rho(T') = \rho(T)\,(1 + \alpha(T - T')) \tag{2.1}$$

Then, one has:

$$\rho_i(T_i) = \rho_o\,(1 + \alpha\beta z)$$

The mass conservation equation

$$\frac{\partial}{\partial t}\,\delta\rho + \operatorname{div}(\rho \underset{\sim}{V}) = 0$$

written to first order in fluctuations leads to:

$$\frac{\partial}{\partial t}\,\delta\rho + \rho_i \operatorname{div}(\underset{\sim}{V}) + \underset{\sim}{V}.\underset{\sim}{\nabla}(\rho_i) = 0$$

where $\delta\rho = \rho(T_i + \delta T) - \rho(T_i) = -\rho(T_i)\alpha\delta T$ and $\underset{\sim}{V}$ is the fluid velocity. Using equation (2.1), this gives:

$$\delta\rho = -\rho_o\alpha(1 + \alpha\beta z)\,\delta T$$

The two terms $\frac{\partial}{\partial t}\,\delta\rho$ and $\underset{\sim}{V}\cdot\underset{\sim}{\nabla}(\rho_i)$ are both linear in α and in the fluctuations: they can be neglected. This leads to:

$$\operatorname{div}\,\underset{\sim}{V} = 0$$

and justifies the fact that, in the following equations, we shall only keep the V_z component of the velocity.

Heat conduction equation The conservation equation of the entropy s:

$$\frac{\partial}{\partial t}(\rho s) = -\operatorname{div}(\rho s \underset{\sim}{V}) - \operatorname{div}(\underset{\sim}{J}_s) + \Sigma$$

may be written as:

$$\rho T \frac{ds}{dt} = -T \operatorname{div}\left(\frac{\underset{\sim}{q}}{T}\right) + T\,\Sigma \tag{2.2}$$

where the heat flux $\underset{\sim}{J}_q$ is related to the entropy flux $\underset{\sim}{J}_s$ by:

$$\underset{\sim}{J}_q = T\underset{\sim}{J}_s$$

Let us recall the expression of the viscous stress tensor[†11]

$$\overline{\overline{\sigma}}' = \alpha_1(\underset{\sim}{n}\,\overline{\overline{A}}\,\underset{\sim}{n})\underset{\sim}{n}\,\underset{\sim}{n} + \frac{\gamma_2-\gamma_1}{2}\,\underset{\sim}{n}\,\underset{\sim}{N} + \frac{\gamma_2+\gamma_1}{2}\underset{\sim}{N}\,\underset{\sim}{n} + \alpha_4\,\overline{\overline{A}} + \alpha_5\,\underset{\sim}{n}(\underset{\sim}{n}\,\overline{\overline{A}}) +$$

$$\alpha_6\,(\overline{\overline{A}}\,\underset{\sim}{n})\underset{\sim}{n} \quad \text{where } A_{ij} = \frac{1}{2}(V_{i,j} + V_{j,i})\,;\ \underset{\sim}{\omega} = \frac{1}{2}\underset{\sim}{curl}\,\underset{\sim}{V},\ \underset{\sim}{N} = \frac{d\underset{\sim}{n}}{dt} - \underset{\sim}{\omega}\Lambda\,\underset{\sim}{n}$$

The entropy source $T\Sigma$ is defined as:

$$T\Sigma = -\underset{\sim}{J}_s.\underset{\sim}{\nabla}T + \vartheta \tag{2.3}$$

where the dissipation ϑ is:

$$\vartheta = \sigma'_{ij}\,V_{j,i} + \omega_i\Gamma_i$$

and the torque Γ is:

$$\underset{\sim}{\Gamma} = \underset{\sim}{n}\,\Lambda\,\underset{\sim}{h},\ \underset{\sim}{h} = -\frac{\delta\mathcal{F}}{\delta\underset{\sim}{n}}$$

In this espression the free energy $\mathcal{F}$ includes, in addition to the Frank[13] elastic term F_{el}, terms due to external fields F_{ext} such as the magnetic field

$$\mathcal{F} = \int (F_{el} + F_{ext})\,dv$$

$$F_{el} = \frac{1}{2}(K_1\,(\text{div}\,\underset{\sim}{n})^2 + K_2(\underset{\sim}{n}.\underset{\sim}{\text{curl}}\,\underset{\sim}{n})^2 + K_3(\underset{\sim}{n}\Lambda\,\underset{\sim}{\text{curl}}\,\underset{\sim}{n})^2)$$

(the distortion studied here involves only the bend elastic constant K_3). The dissipation, which includes only second order terms in the fluctuations, gives no contribution to Eq. (2.3).

---

† We use the following notations:

$\underset{\sim}{a}\,\underset{\sim}{b}$ is a dyadic with the components $(a\,b)_{ij} = a_i b_j$, $f_{,i} = \dfrac{\partial f}{\partial x_i}$

(Div $\overline{\overline{T}}$) is a vector with components $(\text{Div}\,\overline{\overline{T}})_i = \sum_j T_{ji,j}$

The heat flux $\underset{\sim}{J}_q$ is expressed in terms of the thermal conductivity tensor $\bar{\bar{k}}$ and the thermal gradient as:

$$\underset{\sim}{J}_q = -\bar{\bar{k}}\,\underset{\sim}{\nabla} T \tag{2.4}$$

then, using Eq. (2.4) and (2.3), one obtains the heat conduction equation:

$$\frac{\partial}{\partial t}\delta T - \beta V_z + \kappa_{//} k^2 \delta T + \kappa_a \beta \psi = 0 \tag{2.4}$$

where $\psi = \dfrac{\partial \phi}{\partial x}$ is the curvature of the bend distortion and β is $-\nabla_z T$.

Angular momentum conservation The angular momentum conservation leads to the torque balance equation:

$$\underset{\sim}{n} \Lambda \underset{\sim}{h} + \underset{\sim}{\Gamma}_{\text{vis}} = 0 \tag{2.5}$$

The viscous torque Γ_{vis} is expressed in terms of the Leslie-Ericksen viscous stress tensor σ' as:

$$\Gamma_{i\,\text{vis}} = \epsilon_{ijk}\,\bar{\bar{\sigma}}'_{jk} = -\,\underset{\sim}{n} \Lambda (\gamma_1 \underset{\sim}{N} + \gamma_2 \bar{\bar{A}}\,\underset{\sim}{n}) = \gamma_1 \left(\frac{\partial \phi}{\partial t} - \frac{\gamma_1 - \gamma_2}{2\gamma_1}\frac{\partial V_z}{\partial x}\right);$$

Equation (2.5), written to first order in ϕ, gives:

$$K_3 k^2 \phi + \gamma_1 \left(\frac{\partial \phi}{\partial t} - \frac{\gamma_1 - \gamma_2}{2\gamma_1}\frac{\partial V_z}{\partial z}\right) = 0 \tag{2.6}$$

Acceleration equation The equation of motion, given from the conservation of the linear momentum is:

$$\frac{\partial}{\partial t}(\rho \underset{\sim}{V}) = -\,\text{Div}(\rho \underset{\sim}{V}.\underset{\sim}{V}) + \text{Div}(\bar{\bar{\sigma}}^e + \bar{\bar{\sigma}}') + \rho \underset{\sim}{F} \tag{2.7}$$

$\bar{\bar{\sigma}}^e$, the elastic stress tensor defined in Ref. (11) gives no first order contribution to Eq. (2.7). The external force is:

$$\rho F_i = \rho g \alpha \delta T\, \delta_{iz}$$

where g is the gravity acceleration.

Equation (2.7) defines, to the zero order in ϕ, the pressure and gives, to first order in ϕ :

$$\rho \frac{\partial V_z}{\partial t} = \rho g \alpha \delta T + \frac{\gamma_2 - \gamma_1}{2\gamma_1}\frac{\partial \Gamma}{\partial x} + \eta' \frac{\partial^2 V_z}{\partial x^2} \tag{2.8}$$

where the viscosity η' is:

$$\eta' = \frac{\gamma_1(2\alpha_4 + \alpha_5 + \alpha_6) - \gamma_2^2}{4\gamma_1}$$

Instability threshold

The thermohydrodynamic behavior of the system is described by the Eqs. (2.4, 6, 8). The roll instability corresponds to positive values of the time constant s^{-1} (s real). Then the threshold is obtained by solving the system (2.4, 6, 8) for $s = 0$. The calculation leads to a threshold

$$\nabla_{CL}T = \frac{\cdot \nabla_I T}{1 + a\,\kappa_a\,\tilde{T}k^2} \tag{2.9}$$

where $\nabla_I T$ is the Benard critical value for an isotropic liquid:

$$\nabla_I T = -\frac{\kappa_{//} k^4 \mu}{\rho g \alpha} \tag{2.10}$$

with a viscous coefficient $\mu = \eta' + \frac{(\gamma_2 - \gamma_1)^2}{4\gamma_1}$

(the critical Rayleigh number $R_a = 1740$ is obtained for an optimum wave number $k \simeq \frac{2\pi}{d}$).

Indeed, in an isotropic liquid, the instability exists only if $\nabla_I T$ is negative (this is obtained when the sample is heated from below).

In a LC such as MBBA (where $\kappa_a \simeq 10^{-3}$ cgs), the term $a\,\kappa_a \tilde{T}k^2$ in the denominator of 2.9 gives a large contribution:

$\tilde{T} = \frac{\eta_B}{K_3 k^2}$ is the relaxation time of the distortion of the LC in the absence of a field[14] with the bend viscosity

$$\eta_B = \frac{\gamma_1(2\alpha_4 + \alpha_5 + \alpha_6) - \gamma_2^2}{\gamma_1 - 2\gamma_2 + 2\alpha_4 + \alpha_5 + \alpha_6}$$

as defined in Ref. 15.

Using the expression of the viscosity ratio $a = \frac{\gamma_1 - \gamma_2}{2\eta_B}$, the expression (2.9) may be written as:

$$\nabla_{CL}T = \frac{\nabla_I T}{1 + \frac{\kappa_u}{K_3}\,\kappa_a\,\frac{\gamma_1 - \gamma_2}{2}} \tag{2.11}$$

With typical values of γ_1 (0.76 Poise), γ_2 ($-$ 0.79 Poise), K_3 (10^{-6} cgs)[1],we obtain $\frac{\kappa_a}{K_3}\frac{\gamma_1-\gamma_2}{2} \simeq 10^3$

1) if $\kappa_a > 0$, one expects convective instabilities only for $\nabla T < 0$. Ignoring the effect of the cell boundaries, the above one dimensional analysis predicts an approximate reduction of the critical threshold ∇T_{cr} by a factor of 10^3 with respect to the isotropic case.

2) for $\kappa_a < 0$, expression (2.9) shows that convective instabilities can only exist if $\nabla T > 0$.

An explanation of the result of formulae (2.10 and 11) can be obtained by expressing the inequality threshold in terms of some characteristic times:

$$\frac{\tau_{\text{cond}//}}{\tau_{\text{conv}}}\left(1 + \frac{\widetilde{T}}{\tau_{\text{anis}}}\right) > 1 \tag{2.12}$$

$\tau_{\text{conv}} = \frac{\mu k^2}{(-\nabla T)\rho g \alpha}$ and $\tau_{\text{cond}//} = \frac{1}{\kappa_{//} k^2}$ are the characteristic times of the two processes (convection and heat diffusion) which exist in an ordinary liquid.

$\tau_{\text{anis}} = \frac{1}{a\kappa_a k^2}$ is the characteristic time of the anisotropic mechanism (creation of warmer and cooler regions due to the director fluctuation). The condition (2.12) expresses the fact that the instability can set up only if the characteristic times of the stabilizing processes (heat diffusion, liquid crystal relaxation) are larger than the times corresponding to destabilizing processes (convection, anisotropic mechanism).

If one applies a value $\Delta T = 0.5°$K in a MBBA sample of 1 mm thickness, one obtains $\tau_{\text{conv}} \simeq 20$s, $\tau_{\text{cond}//} \simeq 1$ s, $\tau_{\text{anis}} \simeq 1$ s, $\widetilde{T} \simeq 200$ s. These values correspond to the assumption $k \simeq \frac{\pi}{d}$). The convection condition (2.12) is then satisfied for such a LC sample. In an isotropic liquid of the same thickness, the condition would reduce to the inequality $\frac{\tau_{\text{cond}//}}{\tau_{\text{conv}}} > 1$ which is not satisfied for the set of parameters just defined.

Finally let us point out that the convective threshold can be modified by applying a magnetic field which changes the relaxation time of the structure $\widetilde{T}$.[14]

In the presence of a magnetic field $H_\perp$ perpendicular to the plates, the relaxation time

$$\widetilde{T} = \frac{\eta_B}{K_3 k^2 - X_a H_\perp^2} \tag{2.13}$$

is increased. The magnetic field $H_\perp$ is destabilizing and lowers the threshold:

$$\nabla T(H_\perp) = \nabla T(H = 0)\ (1 - \frac{H_\perp^2}{H_c^2}) \tag{2.14}$$

where H_c is the Freedericksz critical field $H_c = \frac{\pi}{d}\sqrt{\frac{K_3}{\chi_a}}$

χ_a is the magnetic susceptibility anisotropy. In a parallel-stabilizing-field $H_{//}$, we obtain similar results to (2.13, 14) by changing $H_\perp^2$ by $- H_{//}^2$.

EXPERIMENTS

We will discuss here essentially the qualitative features of the convection. A quantitative determination of the threshold requires the measurement of the change in effective heat conductivity across the LC above R_{cr}. This cannot be done accurately with the "open" structure used in our optical measurements. In addition, the time constant for appearance of convection is long, close to the threshold (the value R_{cr} *is characterized by an infinite time* constant s^{-1}) and a dynamical description should be made. This will be the object of an independent report.

Geometry

The geometry of the optical cell is shown on Figure 3. The LC film is contained between two transparent circular plates ($\phi = 6$ cm) separated by spacers of well-controlled thickness ($d = 500\ \mu$ to 2 mm with a thickness definition of the order of 1 μ). The planar alignment was obtained by polishing the plates: we use lucite plates rubbed along one axis with a plastic polishing compound and we obtain thick films giving the perfect conoscopic image of a uniaxial crystal. An alignment of

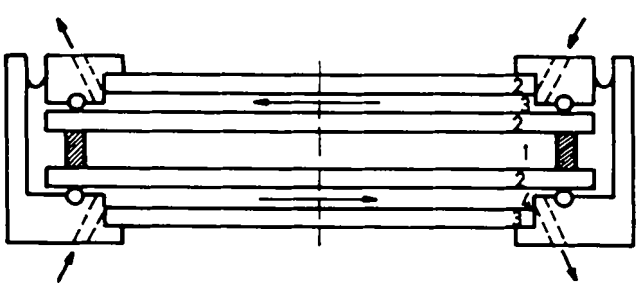

FIGURE 3 Schematic of the thermal cell: 1, liquid crystal, 2, transparent glass or plastic plates, 3 and 4, cold and hot circulating water.

equivalent quality could not be obtained with polished glass cells of the same thickness. The temperature gradient was maintained with a stability of 0.1°C by circulating cold and hot water on the two external sides of the plates. The aspect ratio of the cell was large enough to have a central part of the optical field independent of the edge effects.

Observations

We consider here only experiments with temperature differences close from the threshold values, which correspond to the theoretical treatment. In larger temperature gradients, the structures become progressively more complex (non linear effects) as is also found in isotropic fluids.

If the heat is applied from above, no distortion of the LC can be obtained up to the largest temperature gradient available (30°C). If the heat is applied from below, distortion appears above a certain threshold ΔT_{cr}.

A typical series of observations in a large enough temperature gradient is shown in Figures 4-7 for a 500 μ thick film. The applied temperature difference is $\Delta T = 18.6$°C whereas the measured threshold is $\Delta T_{cr} = 15.5$°C. Similar results were obtained on a 1 mm thick cell with a correspondingly reduced temperature gradient.

– The convection usually nucleates as pairs of convection cells around defects of the structure (Figure 4). This is clearly due to the strong thickness dependence as well as to the elastic distortion already present around such

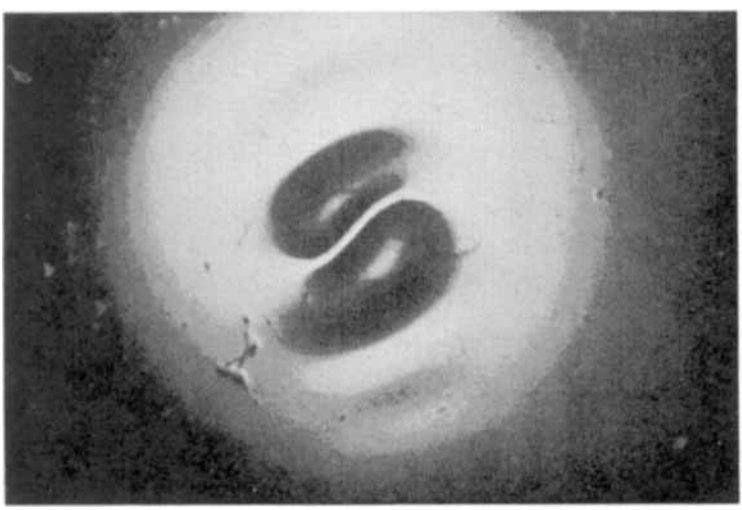

FIGURE 4 The convection initially appears as a pair of rolls of opposite calculation.

points. The growth time of a cell was typically of the order of 1 h when close from ΔT_{cr}.

– For larger times, a periodic roll structure develops (Figure 5). The axis of the rolls is perpendicular to the initial orientation of the LC. The structure is not observed in a light polarized perpendicular to the optical axis. These facts indicate indeed that the convection is directly connected with the orientation of the LC. The analogy between this structure and the Williams electrohydrodynamic domains[17] is striking as is the parallelism between the theoretical descriptions of these two effects. However, unlike the Williams domains observed in thinner films through the formation of optical focals, the observations are made here by direct observation. A characteristic feature of the observation is the existence of a double periodicity in the cell structure. The same effect is seen on Figure 7 showing a larger number of rolls. This turned out to be due to a small misalignment of the cell with respect to the horizontality. A discussion of the physics of this effect will be given independently. In order to characterize more precisely the structure, we have applied two other techniques.

Topographic image An image of the LC deformation can be obtained by illuminating the cell under a wide coherent monochromatic beam perpendicular to the glass plates. Crossed polarizer and analyzer at 45° with the initial director axis are used. An interference pattern due to the change of birefringence in different regions of the cell can be observed. Figure 6 gives such an image corresponding exactly to the rolls of Figure 5. The sharp bright maxima of intensity of Figure 5 correspond to undistorted regions ($\phi = 0$). The birefringence is stationary

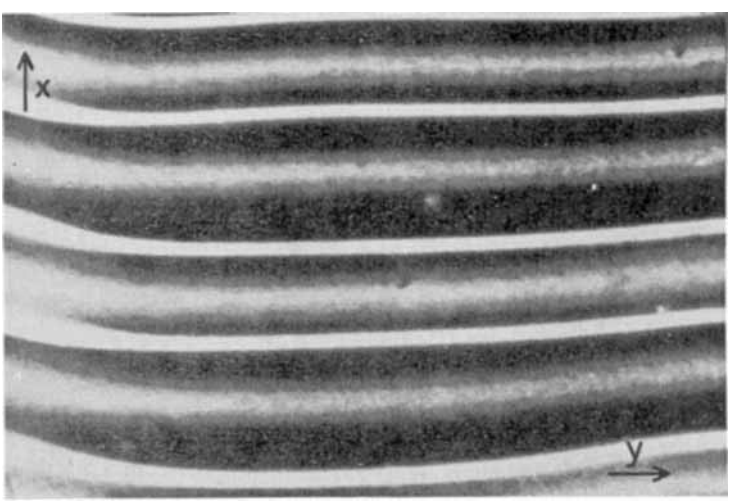

FIGURE 5 Well-developed convection. The axis corresponds to those of Figure 1.

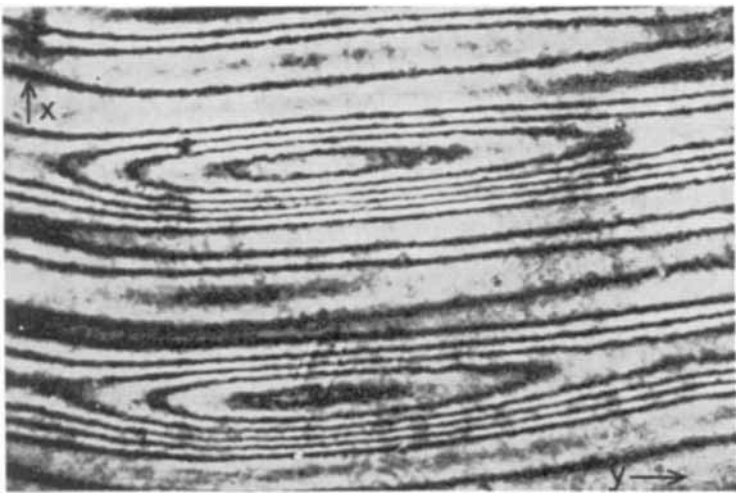

FIGURE 6 Using coherent monochromatic parallel light, a topographic image of the rolls of Figure 2 is obtained.

if one moves along Ox and Oy starting from these lines. These bright lines thus correspond to the boundary lines between two convection rolls. The variation of the birefringence is also small around the half way lines corresponding to inflexion points in the curvature (ϕ extremum). The count of interference fringes gives an indication of the distortion. If one assumes a sinusoidal variation of ϕ along Oz, $\phi = \phi_m \cos\frac{\pi z}{d}$, with a small enough value of ϕ_m the number N of fringes counted from the lines of maximum birefringence ($\phi = 0$) to the regions of maximum distortion is:

$$N = \frac{d}{4\lambda} n_o \left(1 - \frac{n_e^2}{n_o^2}\right) \phi_M^2$$

This gives values $\phi_M = 16^\circ$ and 9° for the larger and the smaller periods. In fact, the topographic image can be used to observe the onset of instability (a distortion ϕ_M of the order of 2° can be detected) more accurately than direct vision with a reduced contrast.

Thermal image If a small horizontal temperature gradient is introduced, when the temperature of the upper plate is close from the critical temperature of MBBA, Tc, a thin interfacial layer can be created in a region of the field of vision. When the limit of the interface, which is essentially the isothermal line $T = T_c$, crosses the convection rolls, it develops a zig zag structure, due to the temperature modulation, at right angle with the rolls. The hot lines correspond to the points of

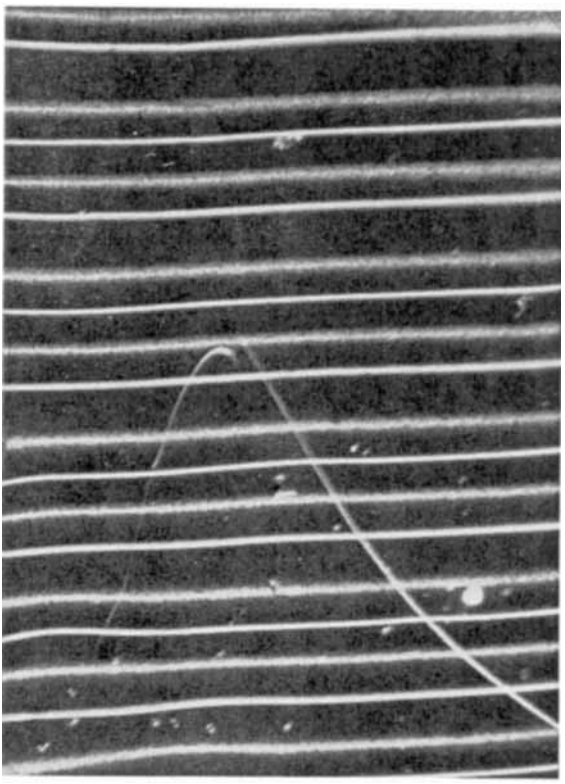

FIGURE 7 Regular array of rolls.

largest penetration of the interface in the nematic. Such a structure is shown on Figure 8 together with a schematic representation of the cell and orientation pattern. The shadows which reveal the curvature of the rolls have been produced by slightly inclining the parallel beam of light. The roll structure extends in the region with an interface. A more detailed description of the interfacial properties will be discussed later.[18]

Quantitative measurements The wavelength of the cell pattern λ was of 1.15 ± 0.05 mm for the 500μ thick cell and 1.9 ± 0.1 mm for the 1 mm one. These values are compatible with the choice $kd = \pi$ or $\lambda = 2d$ used in the theoretical analysis.

The temperature threshold ΔT_{cr} (H=0) is of 15.5° for $d = 500\ \mu$ and 2.3° for $d = 1$ mm. This is consistent with the d^{-3} dependence. The absolute values agree reasonably well with the theoretical estimate.

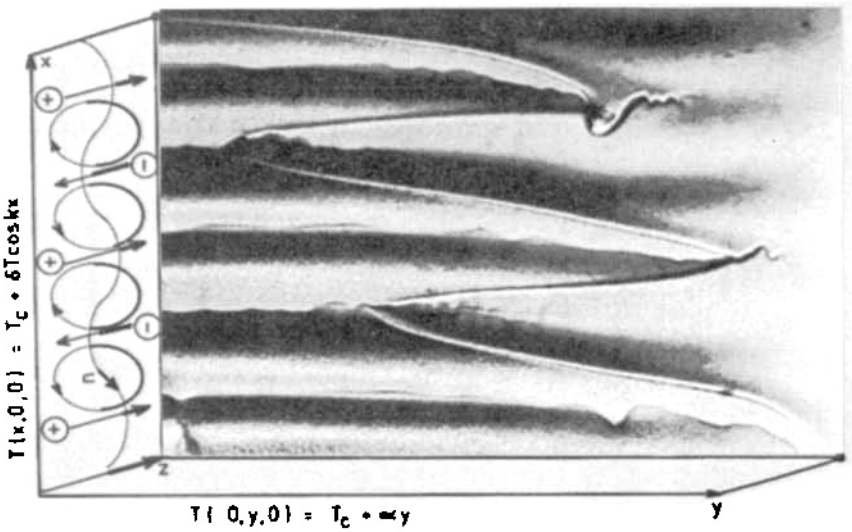

FIGURE 8 The lower temperature is close from T_C and the temperature gradient has a small component along Oy. The wavy shape of the limit between the regions with (left part) and without (right part) an interface allows an estimate of the horizontal modulation of temperature in the presence of convection.

Magnetic field dependence

In order to study the magnetic field dependence of the threshold, we have replaced the parallel wall cell by a wedge geometry. The thickness was varied typically by a factor of 2 ($d \simeq 1$ mm to 500 μ) over the length of the cell. The axis of the wedge was perpendicular to the molecular axis. A schematic description of the set up is shown in the insert of Figure 9. The results of a typical experiment were presented on a slow motion movie in the 1972 Kent Liquid Crystal meeting. The limit between the thinner undisturbed regions and the thicker ones where convection is observed is very sharp because of the strong dependence of ΔT_{cr} with d. The dependence of the temperature threshold with a stabilizing field $H_{//}$ and destabilizing field $H_{\perp}$ was observed from the displacement of the border line. The results of the observations are summarized in Figure 9. The time interval between two consecutive measurements was larger than 10 h to make sure that a stable state had been reached.

In zero field, the critical thickness is found to decrease as the temperature difference between the plates increases. The critical thickness is deduced from the position of the boundary line identified by index 1 to 5 on the cell (1 corresponds to the smallest thickness).

The effect of a stabilizing $-H_{//}-$ and destabilizing $-H_{\perp}-$ field is shown on the same diagram with $H_{//}^2$ plotted along the positive x axis and $H_{\perp}^2$ along the negative one. In agreement with the preceeding results (formulae (2.13) and (2.14)), we find: 1) ΔT_{cr} increases linearly with $H_{//}^2$ and decreases linearly with $H_{\perp}^2$, 2) the // and $\perp$ variations define a single law, 3) the extrapolation of ΔT_{cr} to zero should give the value of the Freedericksz critical field. This has been checked by comparing with independent measurements of H_c.[1]

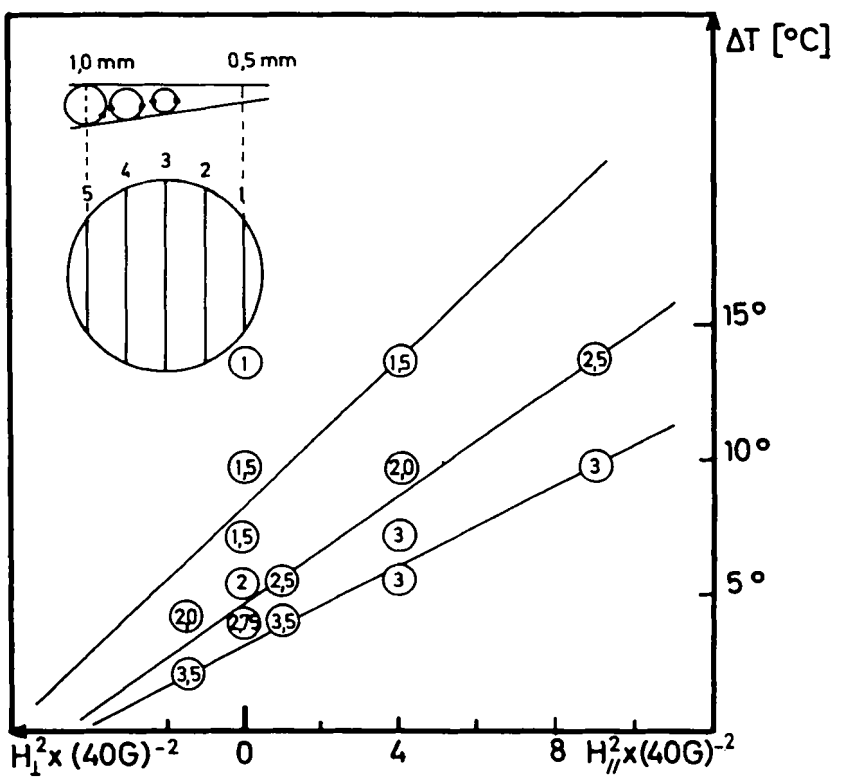

FIGURE 9 The insert shows the geometry of the wedge shaped cell and the index numbers refer to equidistant lines. The limit of the convective domain is measured with respect to these lines. For a given position of this limit (constant index), i.e. for a given thickness, the temperature threshold increases in a parallel field and decreases in a perpendicular one as H^2. It vanishes at the Freedericksz critical field.

CONCLUSION

In conclusion, we have demonstrated both experimentally and theoretically the original features of the heat convection mechanism in a nematic LC film, of positive heat conductivity anisotropy. This provides a clue to the understanding of the orientation effect for such a LC in a vertical thermal gradient.[19, 20] Experiments on materials with a negative heat conductivity anisotropy are desirable. In addition, the use of the LC provides a new approach of the important problem of cellular convection in ordinary liquids:[7] it offers the possibility of studying the convection on very thin layers or with very high Rayleigh numbers. The measurement of the birefringence as well as the use of the strong variation of the physical properties with temperature and of a liquid-liquid phase transition offers original tools to study the topography as well as thermal image of the convection.

Acknowledgements

We wish to thank P. G. de Gennes who initially suggested this study.

References

1. Pieranski, P., Brochard, F. and Guyon, E., *J. Phys.* 7, 681 (1972).
2. Longley-Cook M. and Kessler, J.O., *Mol. Cryst. Liq. Cryst.* 2, 31 5 (1971).
3. Longley-Cook M, Thesis University of Arizona (1972).
4. Stewart G.W., *Phys. Rev.* 69, 51 (1945).
5. Patharkar M., Rajan V. and Picot, J. *Mol. Cryst. and Liq. Cryst.*, to be published.
6. Bénard M., *Rev. Gen. des Sciences Pures et Appliquées* 11, 1261 (1900); 11, 1309 (1900).
7. See Chandrasekhar S., *Hydrodynamic and Hydromagnetic Stability*, Oxford Press (1961).
8. Dubois-Violette E., *C.R.A.S.* 21, 275, 923 (1971); Dubois-Violette E., Thèse d'Etat, Orsay (1971).
9. Guyon, E. and Pieranski, P., *C.R.A.S.* 274, 656 (1972).
10. Carr, E.F., *Mol. Cryst. and Liq. Cryst.* 7, 253 (1969); Helfrich, W., *J. Chem. Phys.* 51, 4092 (1969); 52, 4318 (1970).
11. Dubois-Violette, E., de Gennes, P.G. and Parodi, O., *J. de Phys.* 32, 305 (1970).
12. Boussinesq, J., *Théorie analytique de la chaleur* 2, 172 Gauthier-Villars, Paris (1903).
13. Frank F.C., *Disc. Faraday Soc.*, 25, 19 (1958).
14. Brochard, F., Pieranski, P. and Guyon, E., *Phys. Rev. Letters* 28, 1681 (1972).
15. Groupe Cristaux Liquides d'orsay, *J. Chem. Phys.* 51, 816 (1969).
16. Gähwiller, C., *Phys. Letters* 36A, 311 (1971).
17. Durand, G., Veyssié, M., Rondelez, F. and Léger, L., *C.R.A.S.* 270, 97 (1970); Penz, A., *Phys. Rev. Letters* 24, 1405 (1970).
18. Villanove, R., Mitescu, C., Pieranski, P. and Guyon, E., to be published.
19. While this paper was being typed, we received communication of a preprint by P.K. Currie of an independent study of the orientation of liquid crystals by a temperature gradient. Although the detailed theoretical discussion is more complex than the description given in (8) and developed here, the physical grounds are essentially equiva-

lent. In particular, the predicted value of the instability threshold for a planar film heated from below agrees well with our determination.

20. We have recently studied heat convection in planar films of paraazoxyanisol. The results are very similar to those on MBBA and show a strong reduction of the threshold value as compared with an estimate for the isotropic case. The magnetic film dependence is similar to that presented in Figure 9. This result is consistent with the positive value of κ_a for PAA obtained in Ref. 3.